Transmission Security for Single Kinesthetic Afferent Fibers of Joint Origin and Their Target Cuneate Neurons in the Cat

Gordon T. Coleman, Hong-Qi Zhang, and Mark J. Rowe
School of Medical Sciences, The University of New South Wales, Sydney, Australia 2052

Transmission between single identified, kinesthetic afferent fibers of joint origin and their central target neurons of the cuneate nucleus was examined in anesthetized cats by means of paired electrophysiological recording. Fifty-three wrist joint afferent–cuneate neuron pairs were isolated in which the single joint afferent fiber exerted suprathreshold excitatory actions on the target cuneate neuron. For each pair, the minimum kinesthetic input, a single spike, was sufficient to generate cuneate spike output, often amplified as a pair or burst of spikes, particularly at input rates up to 50–100 impulses per second. The high security was confirmed quantitatively by construction of stimulus–response relationships and calculation of transmission security measures in response to both static and dynamic vibrokinesthetic disturbances applied to the joint capsule. Graded stimulus–response relationships demonstrated that the output for this synaptic connection between single joint afferents and cuneate neurons could provide a sensitive indicator of the strength of joint capsule stimuli. The transmission security measures, calculated as the proportion of joint afferent spikes that generated cuneate spike output, were high (>85–90%) even at afferent fiber discharge rates up to 100–200 impulses per second. Furthermore, tight phase locking in the cuneate responses to vibratory stimulation of the joint capsule demonstrated that the synaptic linkage preserved, with a high level of fidelity, the temporal information about dynamic kinesthetic perturbations that affected the joint. The present study establishes that single kinesthetic afferents of joint origin display a capacity similar to that of tactile afferent fibers for exerting potent synaptic actions on central target neurons of the major ascending kinesthetic sensory pathway.

Key words: **cuneate nucleus; kinesthetic input; joint afferent fiber; paired recording; synaptic transmission; dorsal column nuclei**

Introduction

Some of the earliest reports on the actions of tactile and kinesthetic inputs on the CNS emphasized the much greater sensitivity and efficacy of tactile inputs compared with deep inputs in generating reflex motor output (for review, see Matthews, 1966). The distinction is apparent, for example, between the pinna reflex, in which a small tactile input generated by movement of a single hair can discharge perhaps hundreds of motoneurons to elicit this reflex, and the monosynaptic reflex, the input–output relationships of which show an absence of output until many muscle afferent fibers are activated (Coombs et al., 1955; Lloyd et al., 1955). Furthermore, the distinction has been confirmed in recent studies, even, for example, in microneurography studies in human subjects, in which spike-triggered averaging and EMG recordings have shown that single tactile afferent fibers can exert potent synaptic actions on spinal motoneurons (McNulty et al., 1999), in contrast to the absence of such effects from single muscle afferent fibers (Gandevia et al., 1986).

The capacity of individual tactile afferent fibers to exert potent central synaptic actions also extends to neurons of the major ascending sensory pathways, including those of the spinocervical tract (Brown et al., 1987) and the dorsal column nuclei (DCN). At the DCN relay, we showed that all classes of tactile fibers examined [in particular, the fibers associated with Pacinian corpuscle receptors (PC fibers); the slowly adapting type I (SAI) and type II (SAII) fibers associated with Merkel and Ruffini endings, respectively; and the hair follicle afferent fibers] displayed a high security of transmission when tested in a paired, electrophysiological recording arrangement that enabled the efficacy of transmission to be examined for the synaptic relay between the identified single afferent fiber and one of its central target neurons (Ferrington et al., 1987a,b; Vickery et al., 1994; Gynther et al., 1995; Rowe, 2001; Zachariah et al., 2001).

In the present study, a similar paired recording paradigm has been used to examine the central actions of single kinesthetic afferent fibers, in this case of joint origin, to determine whether any dichotomy exists between tactile and kinesthetic fiber classes in the efficacy of transmission at synaptic linkages formed by single fibers of these classes on neurons of the DCN. The paired recording preparation enabled us to selectively activate and monitor the activity of individual joint afferent fibers in the intact wrist joint nerve (Coleman et al., 1998a) while recording simultaneously with a microelectrode from target neurons in the cuneate division of DCN. Preliminary accounts of this study of joint afferent transmission characteristics have been published previously in abstract form (Coleman et al., 1998b, 1999a).

Materials and Methods

Animal preparation. Experiments were conducted on 40 cats that ranged from 2.0 to 4.0 kg in weight, but with most (29) in the range of 2.5–3.5 kg. Experiments conformed to the *Australian Code of Practice for the Care and Use of Animals for Scientific Purposes*. Anesthesia was induced with sodium pentobarbitone (40 mg/kg, i.p.) or a combination of alfaxalone and alfadolone acetate (18 mg/kg, i.m., in two cats) and maintained with a continuous intravenous infusion of sodium pentobarbitone (~2–3

Received Sept. 26, 2002; revised Dec. 2, 2002; accepted Dec. 13, 2002.

This work was supported by the National Health and Medical Research Council of Australia and the Australian Research Council. We acknowledge the technical assistance of C. Riordan and D. Sarno.

Correspondence should be addressed to M. J. Rowe at the above address. E-mail: M.Rowe@unsw.edu.au.

H. Q. Zhang's present address: School of Chinese Medicine, Hong Kong Baptist University, Hong Kong.

 0270-6474/03/232980-13$15.00/0

$mg \cdot kg^{-1} \cdot hr^{-1}$; overdose administered to terminate experiments). Atropine sulfate (80 μg/kg, s.c.) and dexamethasone phosphate (1.2 mg/kg, i.m.) were administered routinely to reduce respiratory secretions and the risk of cerebral edema, respectively. The trachea was cannulated, as were the femoral artery and vein. Autonomic indices of anesthetic level, including heart rate, blood pressure, and pupillary aperture, were monitored continuously, and the animal's hindpaw was pinched periodically to test for a withdrawal reflex. Rectal temperature was maintained at 38 ± 0.5°C. Electrophysiological recording was terminated if mean blood pressure fell below 80 mmHg. Expired P_{CO_2} was usually ~4% but varied depending on the cat's spontaneous rate of ventilation.

The wrist joint nerve, also known as the articular branch of the dorsal interosseous nerve, was freed from overlying forearm extensor muscles but remained in continuity with the CNS via the deep radial nerve (Tracey, 1979; Coleman et al., 1998a). The dorsal surface of the wrist joint capsule was exposed by removal of the overlying muscle tendons. All other nerves supplying the distal forelimb were transected. The skin flaps created by the forearm incision were stitched to a brass ring, which created a pool that was filled with warm liquid paraffin to protect the exposed tissues.

Procedures for electrophysiological recording. After the head was secured in a conventional stereotaxic frame, the cuneate nucleus was exposed, and recording was undertaken according to methods described previously (Vickery et al., 1994). A silver hook electrode was placed under the fine-caliber wrist joint nerve after it had been freed from associated tissues of the forearm for a distance of up to ~4 cm, and an indifferent electrode was attached to nearby skin. To record simultaneously from the central target neurons of identified wrist joint afferent fibers, penetrations were made with tungsten microelectrodes in a grid-like pattern in the cuneate nucleus, 1–4 mm caudal to the obex, and from ~0.5 to ~2 mm lateral to the midline, in a region that corresponded to the "cluster zone" of the nucleus (Kuypers and Tuerk, 1964; Keller and Hand, 1970). Responses recorded in both the DCN and the wrist joint nerve were fed through conventional amplifier stages, displayed on a digital storage oscilloscope, and stored on magnetic tape and in a laboratory computer.

In seven experiments, a low-impedance (≤0.5 MΩ) microelectrode was inserted into the caudal region of the ventral posterolateral nucleus in the contralateral thalamus for antidromic activation (Darian-Smith et al., 1963) to confirm the cuneothalamic identity for a sample of the wrist joint-related neurons. The stimuli used were 100 μsec electrical pulses, up to ~1 mA in strength.

Activation of wrist joint afferent fibers and their cuneate target neurons. Individual joint afferent fibers, identified initially by gentle probing of the exposed wrist joint capsule with von Frey hairs (~50–200 mg wt in applied force), had well demarcated, punctate receptive fields on the capsule within which just one fiber was activated. The spike waveform observed in the wrist joint nerve recording was examined carefully on an expanded time base of a storage oscilloscope to reveal the details of contour and phase to confirm the selective activation of individual units (Coleman et al., 1998a). Cuneate neurons that received wrist joint input were identified initially after tap stimulation (0.4–0.6 mm amplitude, 3 msec duration) of the joint capsule, and their receptive fields were also mapped by means of von Frey hairs.

Controlled mechanical stimuli were applied to the receptive field foci of wrist joint units on the joint capsule by means of circular probes (250 μm diameter) driven by a feedback-controlled mechanical stimulator (Ferrington et al., 1987a,b; Vickery et al., 1994; Gynther et al., 1995). These focally applied stimuli consisted of static mechanical displacements (1–1.5 sec in duration) or trains of sinusoidal vibration often superimposed on a 1.5 sec step indentation. Because flexion or extension movements of the wrist activated multiple afferent fibers, these forms of natural stimulation could not be used to selectively activate single wrist joint afferent fibers. Although only a minority (~40%) of the joint afferent fibers displayed slowly adapting responses to static focal indentation at the restricted amplitudes (≤400 μm) applied with the 250 μm probes, the dynamically sensitive units could be activated in a sustained way by focal vibration. These vibratory stimuli, which lasted 1 sec, began 300 msec after the onset of a 1.5 sec step indentation (0–200 μm) and ranged in frequency from 10 to 400 Hz, at amplitudes up to 150 μm at frequencies ≤100 Hz or amplitudes up to 100 μm at frequencies >100 Hz. Stimuli were typically delivered at 8–10 sec intervals to allow for recovery of the joint capsule and receptor between stimuli.

Analysis of transmission characteristics for the linkage between single wrist joint afferent fibers and their cuneate target neurons. Stimulus-response relationships were plotted from the impulse rates of each member of the joint afferent–cuneate neuron pair, which enabled the transmission characteristics for the pair to be quantified, particularly the gain of the input–output relationship and the extent to which the linkage was capable of amplification of the peripheral signal. The transmission characteristics were also quantified from modified cross-correlograms (Vickery et al., 1994; Gynther et al., 1995). These response correlation histograms (RCHs) were constructed (see Figs. 2, 6, 7) to examine the temporal relationships of impulse activity evoked in wrist joint afferent fibers and their target cuneate neurons. The cuneate spike occurrences were registered and accumulated in the histogram, which used successive peripherally recorded impulses for spike triggering to reset the histogram to time zero. This analysis allowed a minimum latency to be specified. When a cuneate neuron impulse occurred in the analysis channel, the time to the first preceding peripheral fiber spike that occurred before the minimum latency value was calculated and plotted. This refinement allowed for analysis of the response to stimuli that produced interimpulse intervals in the primary fiber that were shorter than the response latency for the central neuron. From these RCHs, we derived three quantitative measures. First, the transmission security for the linkage was calculated as the proportion of wrist joint afferent fiber impulses that evoked a response in the cuneate neuron; second, the cuneate response latency was obtained as the mean ± SD for the initial peak in the RCH associated with the first cuneate spike in instances of doublet or burst responses; and third, the mean central response (designated mean 2° in Figs. 6, 7) was calculated as a measure of the average spike output from the cuneate neuron in response to each effective input spike.

Transmission characteristics were also quantified for different rates of afferent drive in terms of the cuneate spike output to successive input spikes in the wrist joint afferent fibers. This was done when the afferent fiber responded, at different vibration frequencies, in a regular one-to-one manner (i.e., one impulse discharging on each cycle of the vibration).

Fidelity of temporal patterning in transmission between single wrist joint afferent fibers and their target cuneate neurons. Accurate signaling of dynamic perturbations that involve the joint presumably depends on the retention of temporal precision in the transmission of signals across the synaptic junctions in the central pathways. This issue was examined by an analysis of temporal patterning in the paired responses to focal vibration (as a controlled and defined form of dynamic stimulation that was applied to the joint capsule). The capacity of each member of the pair to respond to the focal vibratory stimulus in a phase-locked or synchronized manner was quantified by the construction of cycle histograms (CHs). From these, the tightness of phase locking was quantified (Mardia, 1972) by calculation of the resultant (R) as a measure of vector strength in the cyclic distribution. Descriptions of the CHs together with the formula for deriving the R values have been given previously (Zachariah et al., 2001).

Values of R range from 0 to 1, with values <0.17 indicating an absence of significant phase preference ($p < 0.05$ for $n = 100$) (Durand and Greenwood, 1965). Values >0.3 indicate a highly significant phase preference in the response ($p < 0.0001$ for impulse counts of $n \geq 100$). R values >0.7 are common in phase-responsive neurons of the auditory (Lavine, 1971; Bledsoe et al., 1982) and tactile (Greenstein et al., 1987; Vickery et al., 1994; Gynther et al., 1995) systems. Temporal dispersion in the CHs was also quantified by calculation of the SD for the distribution of impulse occurrences (see Fig. 8).

Results

Evidence for selective activation of individual wrist joint afferent fibers

For the analysis of cuneate transmission characteristics for single kinesthetic sensory fibers of joint origin, it was essential first to achieve selective activation and monitoring of the activity of in-

dividual joint afferent fibers and then to verify that there were no other active fibers that might have contributed to the observed central responses. Our previous methodological paper (Coleman et al., 1998a) described the suitability of the intact wrist joint nerve preparation for achieving the first of these requirements. However, the arguments establishing that both requirements were met for the present paired recording study are as follows. The selective activation of single joint afferent fibers was achieved with the use of gentle focal stimulation of the joint capsule with fine probes under feedback control. This was possible for several reasons. First, the innervation density for group II endings on the capsule is not so great that multiple units are activated by such stimuli. Second, the receptive fields of individual units are invariably small and punctate (Fig. 1) [Coleman et al. (1998a), their Fig. 2]. Finally, the 250-μm-diameter stimulus probe was sufficiently fine that the low-intensity stimuli could be confined within the receptive field of individual afferent fibers.

The requirement for monitoring the activity of the recruited fiber and verifying the selectivity of its activation was met because of the excellent signal-to-noise ratio achieved with whole-nerve recording from the intact wrist joint nerve. When this fine-caliber nerve was freed from the abductor pollicis longus and other tissues of the forearm for distances of 3–4 cm and placed over a thin sheet of plastic film to improve electrical isolation from adjacent tissues, it was possible to achieve a signal-to-noise ratio of at least 5:1–10:1 (Figs. 2, 3, 4) [Coleman et al. (1998a), their Figs. 2, 3]. This created a clear discontinuity between the "noise" level on the recording trace and the spike activity of any activated group II afferent fiber and ensured that the central responses could not be attributed to afferent impulse activity that was buried in the noise of the recording trace. It was also advantageous for verifying the selective activation of individual joint afferents, to eliminate tonic activity in the wrist joint nerve (Fig. 2) [Coleman et al. (1998a), their Figs. 2, 3]. This was achieved by fixing the wrist joint at an angle of ~150°, because most wrist joint afferents discharge tonically only when the joint is at or near full flexion.

An additional precaution that was taken to eliminate any risk that contaminating inputs might be recruited from beyond the wrist joint nerve itself was to denervate the forelimb apart from the wrist joint nerve itself. This involved sectioning the median, ulnar, musculocutaneous, median musculocutaneous, and superficial radial nerves, together with branches of the deep radial nerve that supply forearm muscles (most of which were removed to expose the dorsal interosseous and wrist joint nerves). Furthermore, any small branches of the dorsal interosseous that supplied the interosseous membrane were cut when the abductor pollicis longus muscle was dissected away from the nerve, thus eliminating any possibility of contamination from Pacinian corpuscle-related fibers from this dorsal side of the interosseous membrane. With these precautions, one could be certain that the only fibers providing input to the cuneate nucleus in response to controlled, low-intensity stimulation of the wrist joint capsule were those that could be monitored in the recording traces from the intact wrist joint nerve.

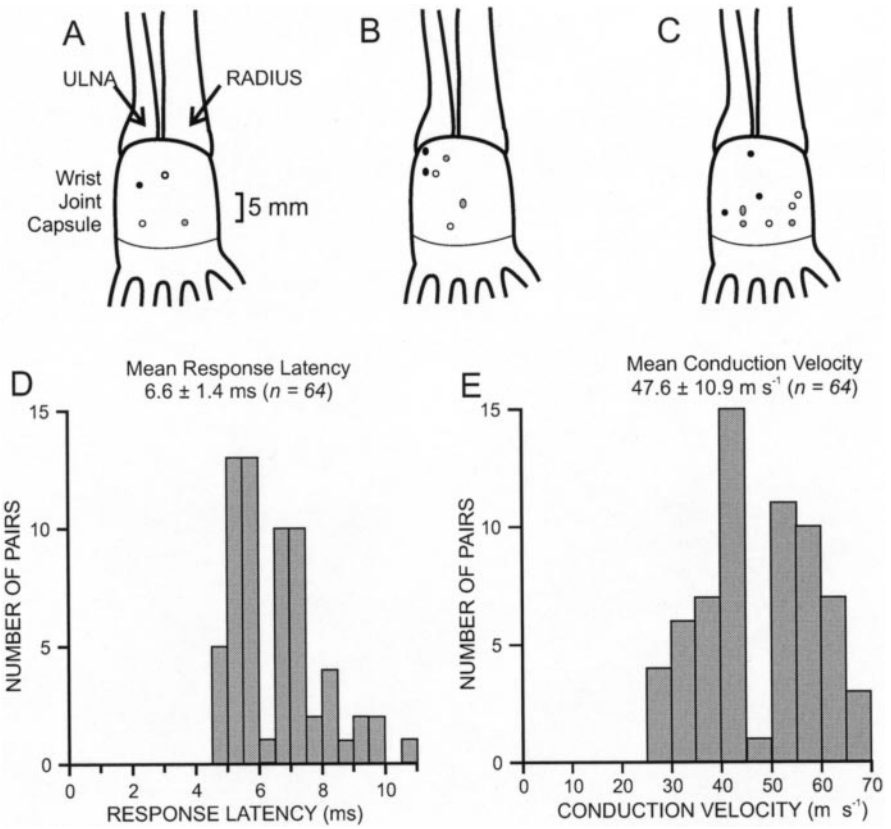

Figure 1. Receptive field, latency, and conduction velocity characteristics for wrist joint afferent– cuneate neuron pairs. Receptive fields are shown in *A* for four neurons activated by probing a single point on the capsule, in *B* for three neurons each activated at a suprathreshold level by two identified afferent fibers from two discrete points on the capsule (*filled*, gray, and *open symbols* for the three pairs of foci), and in *C* for three neurons each activated by three afferent fibers from three discrete foci (*filled*, gray, and *open symbols* for the fields of the three neurons). *D*, The histogram shows the distribution of latencies for cuneate neuron responses to 64 single identified wrist joint afferent fibers measured from the occurrence time of the peripheral spike recorded from the wrist joint nerve in the mid forearm. For each of these latency measurements, the afferent fiber was activated at low rates (~1 Hz). *E*, Distribution of approximate conduction velocities for the wrist joint afferent fibers on the basis of cuneate latency values in *D*, with an allowance of 1 msec for central delay time across the synaptic linkage.

Unequivocal confirmation that the cuneate responses observed in these paired recordings were attributable exclusively to the single monitored joint afferent fiber came from the correlated activity observed in paired impulse traces, such as those of Figures 2–4. Each cuneate response was dependent on previous spike occurrence in the observed joint afferent fiber and followed it at a fixed latency. Furthermore, when the joint afferent fiber failed to respond on some cycles of the vibration stimulus (Fig. 3), there was a correlated failure of response in the cuneate neuron. These response correlations were even more persuasive for nonsynchronizing stimuli, such as the static capsular indentation used to generate the paired responses in Figure 2. In this circumstance, the impulses in the peripheral fiber were evoked irregularly in response to the static displacement, and therefore were not synchronized to any feature of the stimulus. Because the static stimulus cannot synchronize the activity of any other fiber with that of the monitored fiber, we can exclude contributions to this central response from sources other than the monitored fiber.

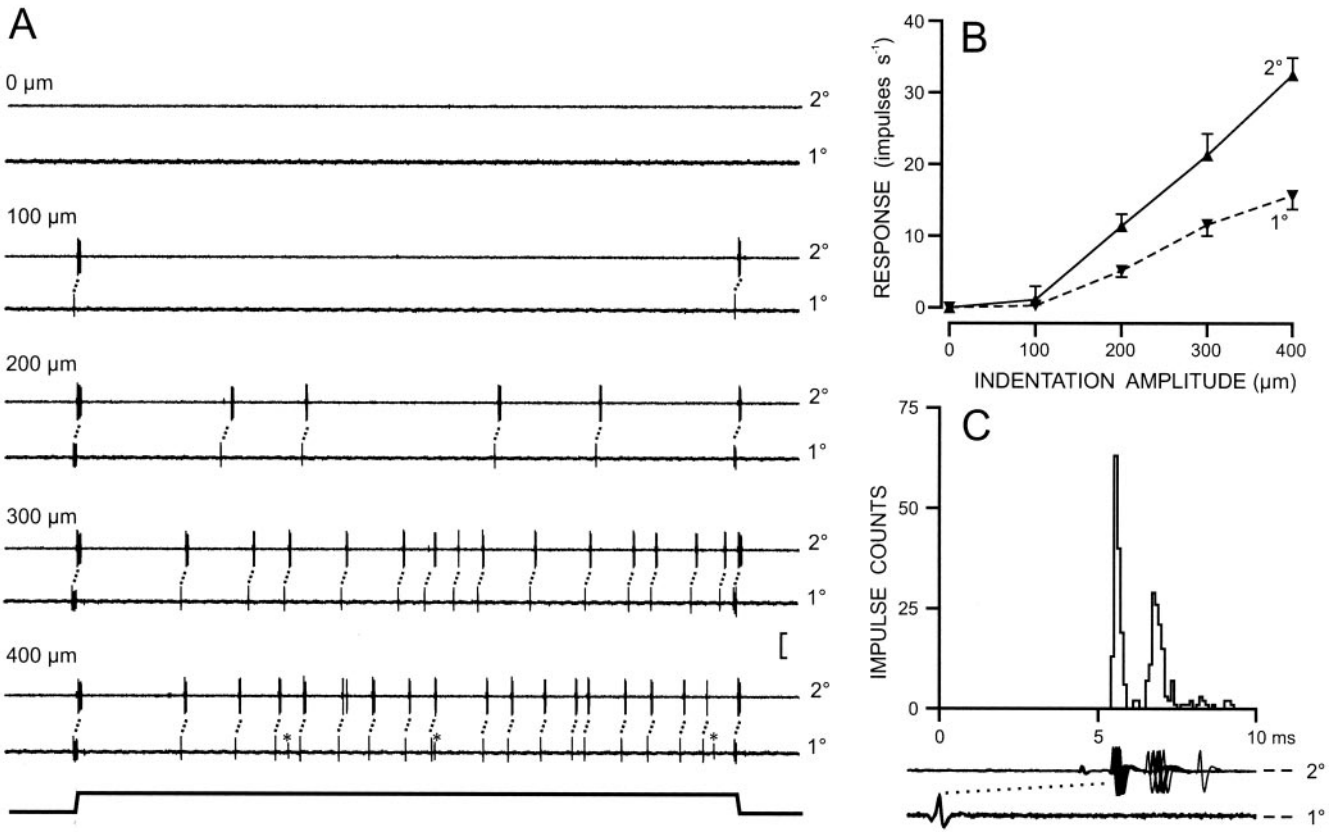

Figure 2. The capacity of single spikes in a wrist joint afferent fiber (1°) to generate spike output from a cuneate target neuron (2°) in response to static indentation of the joint capsule. The paired simultaneous recordings in *A* show the responses to focal static indentation (1 sec duration) of the joint capsule at amplitudes up to 400 μm. The *asterisk* in the peripheral response trace at 400 μm marks the occasional recruitment of a second fiber that fails to elicit any response from this cuneate neuron. Vertical calibration, 0.28 mV for the 1° traces and 0.50 mV for the 2° traces. The stimulus–response relationships in *B* show the graded input–output functions for peripheral (1°) and central (2°) elements (*dashed* and *solid lines*, respectively) and reveal the amplification of output across this synaptic connection. In *C*, the RCH and superimposed impulse traces for 1° and 2° elements illustrate the pairs or bursts of spikes elicited in the cuneate neuron in response to the single input spike. The transient onset segment (~15 msec) of the indentation period was excluded from the impulse counts plotted in *B* and from the RCH in *C* because additional fibers were sometimes recruited by the abrupt onset of the step indentation. In *A* and *C*, the *connecting dots* emphasize the correlation between peripheral and central spike activity.

Representation of wrist joint inputs within the cuneate nucleus

A total of 53 cuneate neurons that could be activated by single identified wrist joint afferent fibers were located in the cluster zone of the cuneate nucleus (Kuypers and Tuerk, 1964; Hand and van Winkle, 1977). All 53 neurons were found between 1 and 3 mm caudal to the obex, 1–1.8 mm lateral to the midline, and at depths of 500–1800 μm within the nucleus. In any one experiment, these wrist joint-related neurons were found in a rostrocaudally oriented column no more than ~250 μm wide at any given rostrocaudal level, in agreement with Millar's (1979) observations for elbow joint input. Because of the extensive denervation performed on the distal forelimb, we did not investigate the extent of any cross-modal convergence (e.g., from cutaneous tactile afferent or muscle afferent fibers) onto this particular joint-related class of kinesthetic neurons.

Receptive fields of cuneate neurons responding to stimulation of the wrist joint capsule

Each of the 53 cuneate neurons studied had discrete, punctate receptive fields that could be delineated clearly by probing the dorsal surface of the joint capsule with fine (50–200 mg wt in applied force) von Frey hairs. Receptive fields were mapped systematically for 39 neurons. Although only a single focus of sensitivity was found on the capsule for most neurons (25 of 39; ~65%; four examples in Fig. 1*A*), a substantial proportion (14 of 39; ~35%) of cuneate neurons responded to stimulation of two or more discrete points on the wrist joint capsule separated by distances of ~1–5 mm. This proportion may be a slight underestimate, because in some cases, the preparation did not allow the entire dorsal surface of the wrist joint capsule to be explored. For seven of these 14 neurons, the receptive fields had two foci (for three examples, see Fig. 1*B*), whereas the other seven neurons had three foci, as shown for three neurons in Figure 1*C*. Each of the separate receptive field foci was small (1–2 mm diameter), either circular or oval in shape, and corresponded in size to the receptive field sizes of individual afferent fibers recorded from the wrist joint nerve. Because the receptive fields for individual wrist joint afferent fibers consisted of just a single point receptive field (Coleman et al., 1998a), the cuneate neurons with dual- or triple-focus fields were activated at a suprathreshold level by two or three convergent joint afferent fibers. The sharply circumscribed nature of the foci and the discontinuity of foci for different peripheral fibers provided one of the persuasive lines of evidence that these cuneate neurons could be activated from each of these foci by quite separate, convergent sensory fibers.

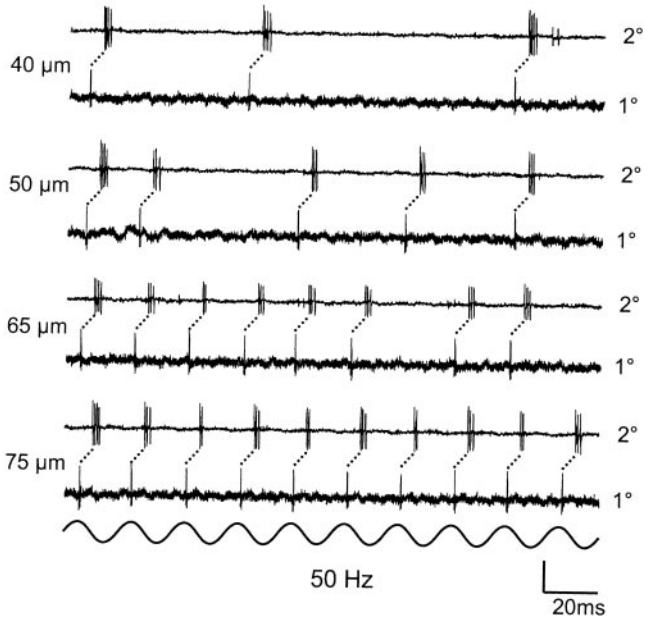

Figure 3. High transmission security and amplification across the connection between a single joint afferent fiber (1°) and a cuneate target neuron (2°) at high rates of afferent drive generated by focal vibration (50 Hz) of the joint capsule at a range of amplitudes (40–75 μm). Where the peripheral fiber failed to respond during a vibration cycle, there was a correlated failure in the response of the cuneate neuron. This close correlation between peripheral and central activity confirmed that the fiber for which activity is shown in the peripheral trace was uniquely responsible for these responses of the cuneate neuron. Vertical calibration, 0.10 mV for the 1° traces and 0.34 mV for the 2° traces.

Responses of cuneate neurons to inputs from single fibers in the wrist joint nerve

Once the receptive field on the joint capsule had been identified for a cuneate neuron, the afferent fiber (or fibers) responsible for generating the central response was identified in the peripheral nerve recording by probing of the joint capsule with a von Frey hair. For each of the 53 cuneate neurons studied, there was a clear correlation between impulse activity that arose in an individual fiber, the activity of which was monitored in the wrist joint nerve, and the response of its central target neuron, even without the use of cross-correlation analysis. The mechanical stimulator probe was then placed over the receptive field of the fiber, and tap stimuli were used to selectively activate the individual joint afferent fiber responsible for generating spike output in the cuneate neuron. For all 53 cuneate neurons, a single action potential that arose in the individual, identified wrist joint afferent reliably produced spike output in the neuron, at least at low peripheral impulse rates.

The mean response latency for cuneate responses from the time of occurrence of the wrist joint afferent spike recorded in the mid forearm, calculated for 64 wrist joint afferent–cuneate neuron pairs (including the responses of some neurons to impulses that arose in two or three separate input fibers), was 6.6 ± 1.4 msec (mean ± SD) and ranged from ~4.7 to 10.9 msec (Fig. 1*D*). An approximate estimate of the overall conduction velocities for the afferent fibers (including peripheral and central segments), based on these latency values and an average conduction distance of 25 cm and allowing 1 msec for an assumed monosynaptic linkage between the afferent fiber and cuneate neuron, gave values (Fig. 1*E*) that fell within the group II range (~30–68 m/sec) for all but four fibers. Although the estimates for the four remaining fibers were slightly lower than the normal group II range (~25–29 m/sec), this is probably attributable to the slower velocity over the central axonal component after entering the spinal cord, where the afferent fiber branches and tapers off after sending axon collaterals to the dorsal horn (Brown, 1968; Clark, 1972; Horch et al., 1976).

Identification of cuneothalamic projection neurons

On completion of the transmission analysis for different joint afferent–cuneate neuron pairs, a small sample of cuneate neurons (five of nine tested) was demonstrated by antidromic activation and collision to have a projection to the region of the contralateral thalamus. This was based on the short-latency (<2 msec) antidromic responses being extinguished by a preceding peripherally evoked spike (Darian-Smith et al., 1963). The proportion of confirmed projection neurons in our sample is likely to be an underestimate, because we used just a single thalamic stimulating microelectrode. Furthermore, all cuneate neurons studied were located within the cluster zone of the nucleus (Kuypers and Tuerk, 1964; Berkley et al., 1986), where the vast majority (>90%) of recorded neurons have been shown to be cuneothalamic projecting neurons (Andersen et al., 1964; Gordon and Jukes, 1964).

Transmission of information about static joint displacement between single joint afferent fibers and their target cuneate neurons

More than one-third (~40%) of the joint afferent fibers that individually generated suprathreshold responses from their recorded cuneate target neurons had slowly adapting responses to static indentation of the joint capsule. In each case, the high transmission security across the linkage enabled the cuneate neuron to respond reliably to each incoming spike elicited by these forms of static, focal indentation of the capsule, which lasted 1 sec (Fig. 2*A*). Because the joint afferent fiber had an approximately linearly graded response as a function of the strength of capsular indentation, this was translated to a similar graded response in the cuneate neuron (Fig. 2*A,B*). Furthermore, at the relatively low rates of afferent drive (usually <20 impulses per second) achieved in the joint afferent fibers by these static displacement stimuli, the individual input spikes often elicited a pair or burst of spikes in the target neuron. Because of the time scale used, this amplification across the linkage is not immediately apparent in the impulse traces of Figure 2*A*. However, such amplification is clear in the stimulus–response relationships of Figure 2*B* and in the RCH of Figure 2*C*. The relationships in Figure 2*B* show the high gain of the transmission process in the form of the steeper slope of the stimulus–response relationship for the cuneate neuron (2°) compared with the joint afferent fiber (1°). On average, there is an approximate doubling of the spike output across the synapse at each indentation amplitude plotted in Figure 2*B* over the focal indentation range of 400 μm. This amplified response, reflected in the doubling of spike output, may provide for a form of temporal summation to ensure secure transmission at the next synaptic junction, in the ventroposterior thalamic nucleus. The RCHs of Figure 2*C*, constructed from five consecutive cuneate responses to the 400 μm stimulus, show the fixed latency (5.6 ± 0.1 msec) for the onset of the amplified, double-spike response relative to the peripheral spike (time 0 on abscissa). The transmission security, calculated as the proportion of joint afferent spikes that evoked any response in the cuneate neuron, was 93%, which reflects the high security of the linkage and the rarity of transmission failures associated with single joint afferent input at discharge rates generated by static joint displacement.

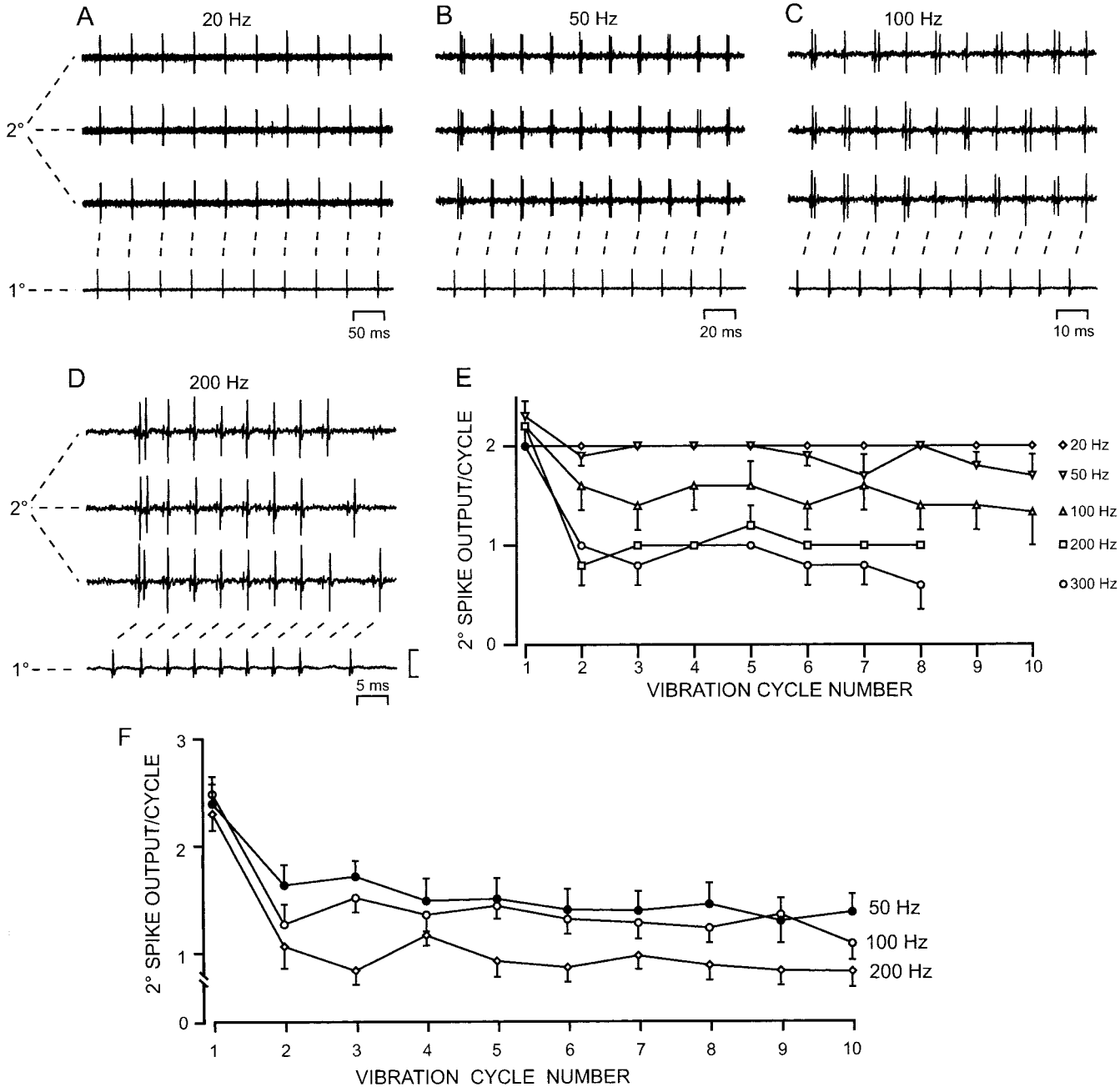

Figure 4. Response traces and quantified output measures for the linkage in wrist joint afferent–cuneate neuron pairs as a function of the frequency and cycle number for focal vibration delivered to the joint capsule. *A–D*, For one pair, one representative trace is shown of the response of the peripheral fiber (1°) and three representative traces are shown for the central neuron (2°) over the first 10 cycles at each frequency from 20 to 200 Hz. At each frequency, the vibration amplitude applied was sufficient to produce a one-to-one following in the fiber over the first 10 cycles, except at 200 Hz, where one-to-one following could only be sustained over the first seven to eight cycles. *E*, Graph of the spike output of this cuneate neuron (2° spike output per cycle) as a function of vibration cycle number when the fiber was driven at a one-to-one level over the first 10 cycles. Each data point represents the mean ± SE response level of the cuneate neuron for five repetitions of the stimulus. At 200 and 300 Hz, a one-to-one response level could not be sustained in the input fiber beyond seven to eight vibration cycles. The vertical calibration in *D* represents 0.10 mV for the afferent fiber traces and 0.20 mV for the cuneate neuron traces. *F*, Security of the linkage for a sample of wrist joint afferent–cuneate neuron pairs quantified as the averaged spike output of the neuron on successive cycles of the focal vibratory stimulus. This measure of cuneate neuron output was obtained at vibratory stimulus frequencies of 50, 100, and 200 Hz for each pair when the wrist joint afferent fiber was responding to the vibration with a regular one-to-one pattern of activity. The mean spike output on each cycle was calculated, up to cycle number 10, and plotted along with SE (error bars). The averaged responses from 14 pairs are shown for the 50 Hz plot and for 15 pairs for the 100 Hz plot. At 200 Hz, the number of pairs that contributed to the plot fell from 11 in each of the first eight cycles to 10 over the last two cycles.

In other pairs studied in this way, there was also evidence of potent amplification across the synaptic connection, with up to four cuneate spikes generated in response to individual joint afferent spikes. Among nine pairs activated by static indentation of the joint capsule, the quantified transmission security values reached 100%, and in all cases, they exceeded 85%.

Transmission security between single joint afferent fibers and cuneate neurons for signaling dynamic features of joint stimulation

Because the response levels generated in individual joint afferent fibers by focal static indentation of the capsule were usually lower (<25 impulses per second) than those reported in response to

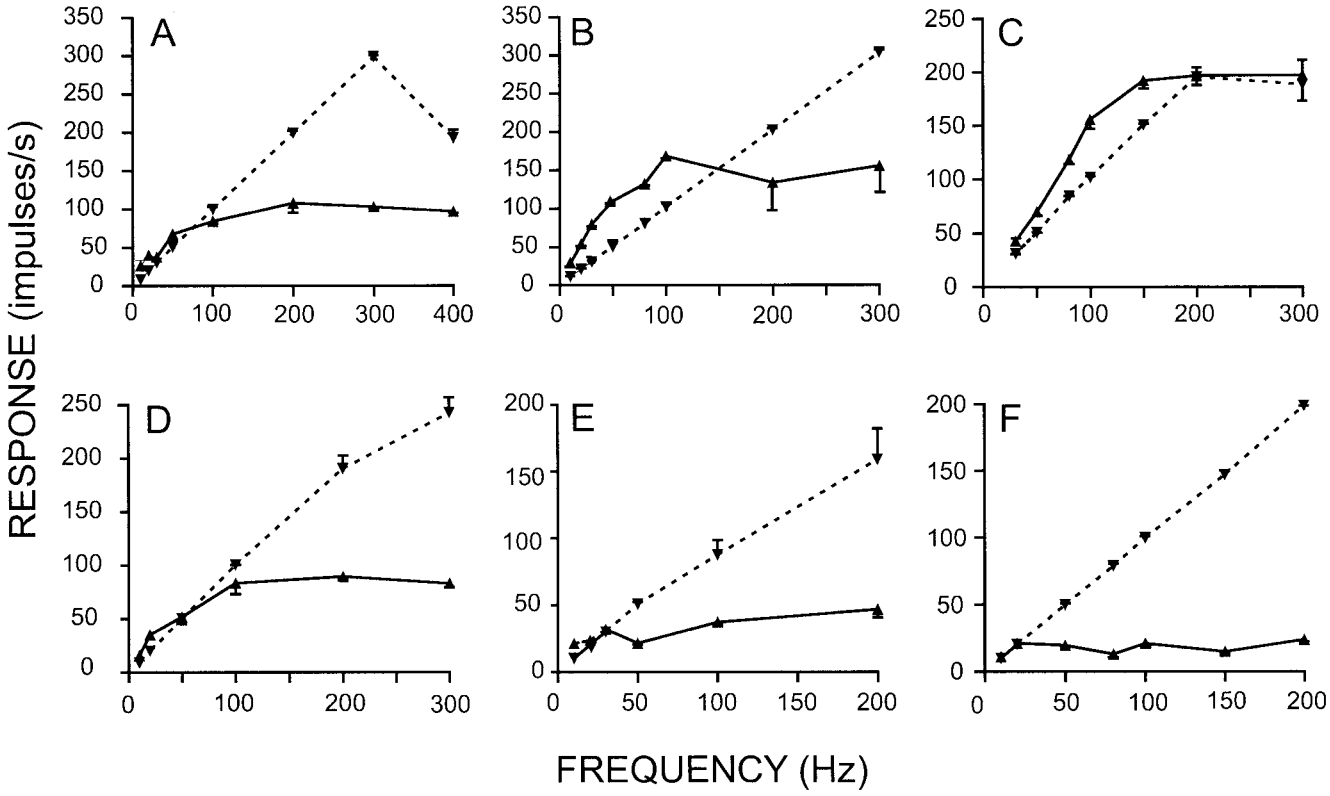

Figure 5. Bandwidth of vibrokinesthetic responsiveness for wrist joint afferent fibers (*dashed lines*) and their target cuneate neurons (*solid lines*). Frequency–response graphs are shown for six wrist joint afferent–cuneate neuron pairs. The response levels plotted at each vibration frequency were for the lowest amplitude that produced a one-to-one (or near one-to-one) impulse rate in the peripheral fiber over the entire 1 sec period of the vibration stimulus. For the six joint afferent fibers in *A–F*, the average vibration amplitudes required for one-to-one firing in the frequency range of 20–200 Hz (where most observations were made and where one-to-one discharge was attained) were as follows: 78 μm at 20 Hz ($n = 6$), 88 μm at 30 Hz ($n = 4$), 77 μm at 50 Hz ($n = 6$), 68 μm at 80 Hz ($n = 3$), 87 μm at 100 Hz ($n = 6$), 70 μm at 150 Hz ($n = 2$), and 77 μm at 200 Hz ($n = 6$). These 33 values ranged from 20 to 140 μm and showed little systematic change as a function of vibration frequency.

maintained joint flexion (Burgess and Clark, 1969; Tracey, 1978, 1979), and because the majority of wrist joint afferents displayed purely dynamic responses to focal capsular indentation, we used sustained forms of dynamic stimuli (in particular, focal vibration at frequencies up to 400 Hz) to examine the transmission characteristics at higher levels of peripheral afferent drive. Furthermore, because the dynamic forms of sensory stimuli generally convey information about change or novelty in the incoming pattern of sensory input, these inputs may be of greater importance in the adaptive behavior of the animal.

The effectiveness of focal vibratory stimuli for generating high levels of synchronized activity in individual joint afferent fibers is shown in the paired impulse traces of Figure 3 in response to 50 Hz vibration at four amplitudes. The linkage for this joint afferent–cuneate neuron pair displays remarkable security and high amplification as the impulse rate in the afferent fiber increases from the low rate at 40 μm to a regular one-to-one pattern (one impulse for each vibration cycle) at 75 μm. Transmission security was 100% at each amplitude of the 50 Hz vibration, because every peripheral impulse elicited a response in the cuneate neuron, and at a consistent latency (Fig. 3).

Transmission characteristics were quantified for 20 joint afferent–cuneate neuron pairs activated by focal vibration of the joint capsule. With systematic variation of the vibration frequency and amplitude, it was possible to generate a regular one-to-one pattern of response in the joint afferent fiber, at least up to impulse rates of ~150–200 per second in most fibers (Fig. 5). Where one-to-one following could not be sustained in the afferent fiber throughout the 1-sec-duration stimulus, the graphs plotted in Figure 5 were for the maximum response rate (≤1:1) attained in the fiber. The input–output relationships plotted in Figure 5 for six representative joint afferent–cuneate neuron pairs (*dashed line* and *solid line*, respectively) show that for four of the six pairs, there was an amplification of input at low rates of afferent drive. However, a crossover or deviation occurred in the graphs (except in Fig. 5*C*) as the response of the central neuron fell below that of its afferent fiber and reached a plateau, ranging from ~20 (Fig. 5*F*) to ~200 (Fig. 5*C*) impulses per second and, in the overall sample of 35 pairs analyzed in this way, from ~20 to 280 impulses per second (113 ± 62 impulses per second; mean ± SD; $n = 35$). Although the data in Figure 5 show the limitations on responsiveness of the central target neurons, it is nevertheless striking that such potent amplification and responsiveness can be sustained across this synaptic relay for the minimum kinesthetic input, that which is derived from a single joint afferent fiber. These highly secure transmission characteristics across the DCN are very similar to those that we observed recently for single hair follicle afferent fibers (Zachariah et al., 2001) and for other tactile fiber classes in previous studies (Ferrington et al., 1987a,b; Vickery et al., 1994; Gynther et al., 1995).

The paired impulse traces in Figure 4*A–D* illustrate directly the potent, high-gain nature of the linkage in response to trains of 10 input spikes at 20, 50, and 100 impulses per second (Fig. 4*A–C*) and the disappearance of amplification in response to the input of 200 impulses per second (Fig. 4*D*). The graphs in Figure 4*E* quantify the mean spike output as a function of vibration cycle

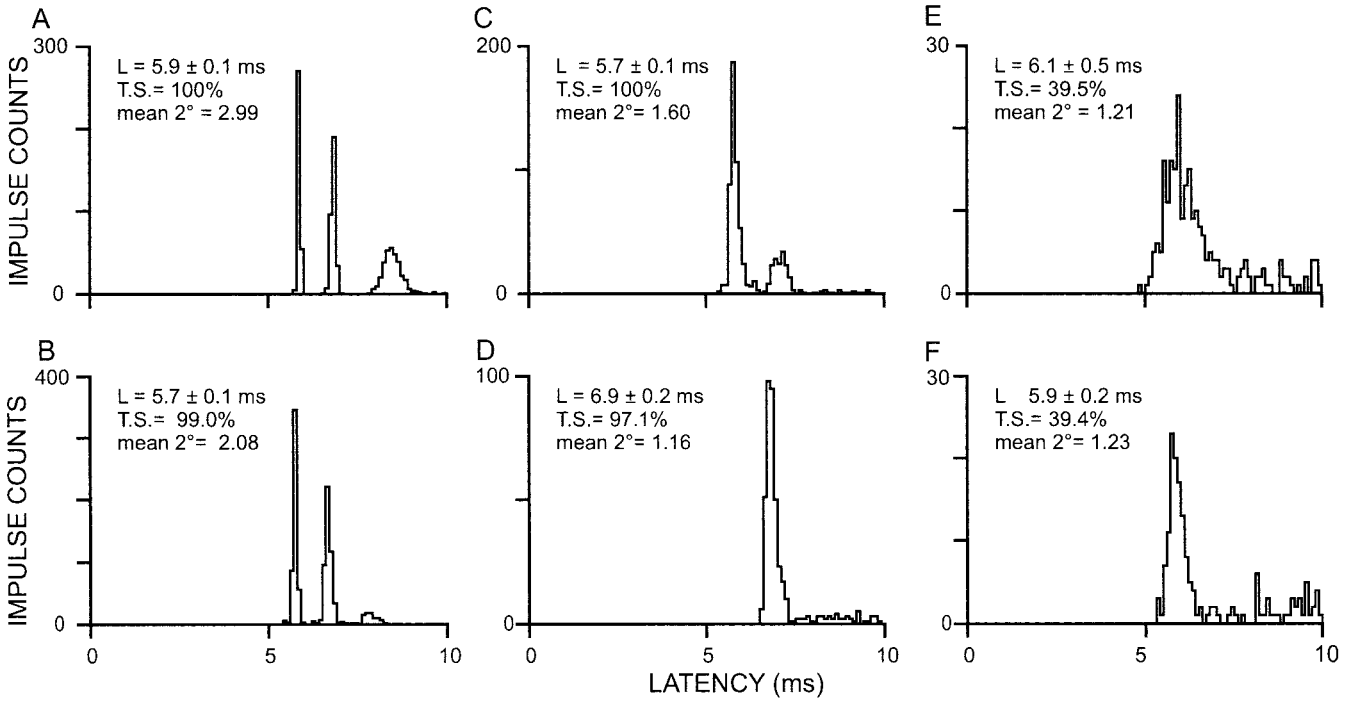

Figure 6. RCHs constructed for six wrist joint afferent– cuneate neuron pairs when the peripheral fiber was driven at a one-to-one or near one-to-one level by a 50 Hz vibration train that lasted 1 sec and that was applied focally to the joint capsule. The security of the linkages for the representative pairs illustrated ranged from transmission security (*T.S.*) values of >95% (*A–D*) to linkages, for which values were ~40% (*E, F*). The mean cuneate response (mean 2°) and its latency (*L*, ± SD) are indicated on each histogram (see Results).

number for this cuneate neuron at five different afferent driving frequencies from 20 to 300 impulses per second. Amplification, reflected in a cuneate spike output of >1.0, was well sustained at 20, 50, and 100 impulses per second over the first 10 cycles. Furthermore, the cuneate response was maintained, albeit without amplification, over these 10 cycles even at the 200 and 300 sec^{-1} driving frequencies. Quantification of the input–output relationships over the first 10 cycles for up to 15 joint afferent–cuneate neuron pairs in Figure 4*F* confirmed the generality of the capacity for sustained amplification in the linkage at input frequencies of up to 100 impulses per second and the potency of transmission even at the 200 sec^{-1} input rate.

With small changes in the position of the central recording electrode to optimize the cuneate neuron recording, there is a second, smaller spike apparent in the 2° traces in Figure 4*D*. We cannot be certain whether this was from a second cuneate neuron activated by the divergent actions of the selectively activated joint afferent fiber or, because it preceded the large cuneate neuron spike, whether it was from the incoming afferent axon.

Quantification of transmission characteristics for responses of joint afferent–cuneate neuron pairs to protracted stimuli

Transmission security over more protracted (1 sec) periods of afferent input was quantified by construction of RCHs that were effectively cross-correlograms (see Materials and Methods) based on the accumulation of the time of occurrence of any cuneate neuron response to each joint afferent spike. This was done for 32 pairs and is illustrated in Figure 6*A–F* for six representative pairs when the afferent spike rate was fixed in each case at 50 impulses per second by means of a 50 Hz focal vibratory stimulus, a rate that may be encountered physiologically in association with joint flexion (Burgess and Clark, 1969; Tracey, 1979). Transmission security was at or near 100% for the four pairs for which the RCHs are illustrated in Figure 6*A–D*. Thus, almost every afferent spike over the 1 sec period of input was effective in eliciting a cuneate response, whereas for the two pairs in Fig. 6*E,F*, the transmission security dropped to ~40%, and with this poorer security, there was greater variability in response latency, in particular in Fig. 6*E*. However, for all six pairs, the cuneate response was amplified, because the mean response (Fig. 6, mean 2°) elicited by each afferent spike exceeded 1.0 and, in Figure 6*A*, was almost 3.0, which indicates a response burst of three spikes per input spike. For the 32 pairs examined at 50 Hz, the mean response per input spike was 1.85 ± 0.55 (SD; range, 1.1–3.0), and the mean transmission security value was 77.5 ± 27 (SD), with more than one-half of the sample (20 of 32) having values of 90–100%.

For most pairs, when the input spike rate was increased above ~50 impulses per second, the transmission security and mean cuneate response level (mean 2°) declined, as has been observed in the transmission characteristics for single tactile afferent fiber classes (Zachariah et al., 2001). Furthermore, there was some increased variability in response latency, as reflected in the values associated with the RCHs obtained for a representative pair in Figure 7*A* when the input rate in the joint afferent fiber was systematically increased by being driven in a one-to-one manner by 50, 100, 200, and 300 Hz vibration trains. In some other pairs, however, as represented in the RCH data in Figure 7*B*, high transmission security was well maintained, along with rather stable values for latency and mean cuneate response, even with input driving rates of 200 and 300 impulses per second.

Temporal patterning in the responses of wrist joint afferent–cuneate neuron pairs

The extent to which the vibration-induced temporal pattern in the joint afferent input was preserved in transmission across the cuneate linkage was quantified by constructing the paired CHs of Figure 8. These histograms, which have an analysis time (abscis-

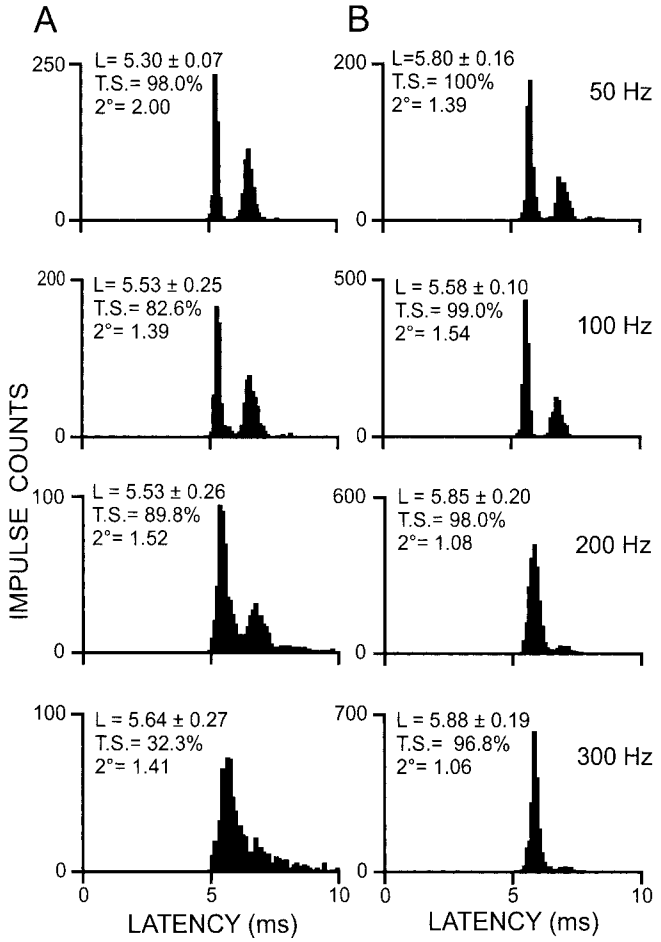

Figure 7. Changes in transmission characteristics for two representative wrist joint afferent– cuneate neuron pairs (*A*, *B*) as a function of increased rates of peripheral drive. RCHs were constructed for each pair in response to focal stimulation of the joint capsule at vibration frequencies that ranged from 50 to 300 Hz. Transmission security (*T.S.*), latency (*L*, ± SD), and mean central response (mean 2°) are indicated on each RCH.

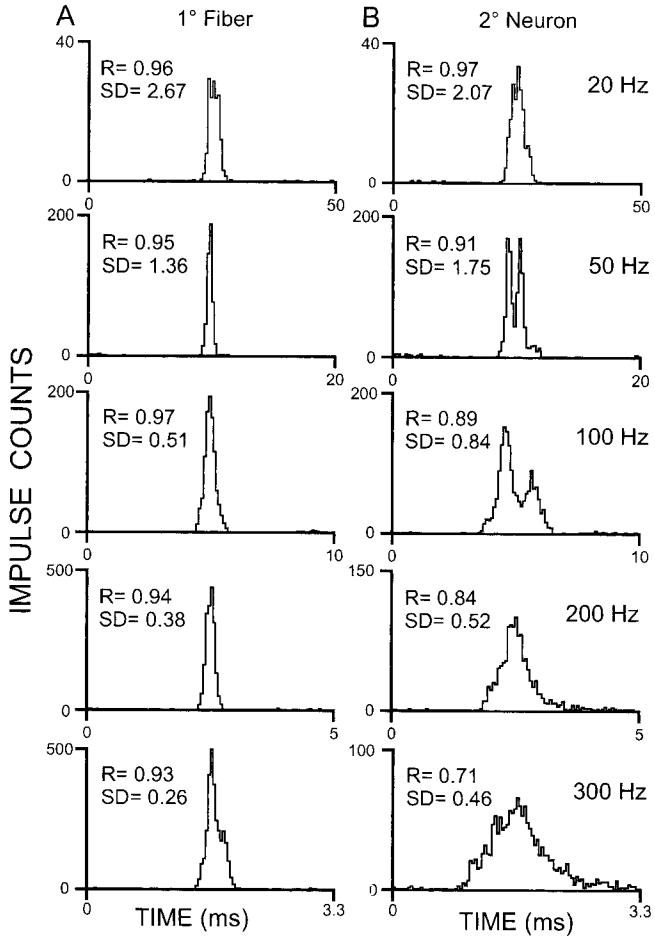

Figure 8. Comparison of the precision of temporal patterning observed in the responses of a wrist joint afferent fiber and its target cuneate neuron to vibration, applied to the receptive field focus on the joint capsule, at several frequencies (20–300 Hz). CHs were constructed from the responses of the fiber (1° fiber) on the left side and the central target neuron on the right (2° neuron). The width of the horizontal axis for each CH corresponds to the duration of one vibration cycle period. Resultant vectors (*R*) and SDs were calculated from the CH distributions of the fiber and its target neuron as measures of phase locking and absolute temporal dispersion, respectively, in the responses of the wrist joint afferent and its target neuron.

sa) corresponding to the cycle period of the particular vibration stimulus, permit direct comparison of the tightness of phase locking in the responses of the input fiber (Fig. 8*A*, 1° fiber distribution) with that of its target neuron (Fig. 8*B*, 2° neuron). They were constructed when the joint afferent fiber was responding to each of the five vibration frequencies (20–300 Hz) with a one-to-one metronome-like impulse pattern, as reflected in the very high vector strengths (*R* values of ≥0.93). The almost identical *R* value for the cuneate response at 20 Hz shows that the temporal precision in the input was preserved in the impulse pattern of the central neuron. The temporal dispersion in the cuneate responses exceeded that of the input fiber at higher vibration frequencies, reflected in the lower *R* values. However, even at 300 Hz, the temporal patterning in the input signal ($R = 0.93$) was remarkably well preserved in the process of synaptic transmission to the cuneate neuron ($R = 0.71$). This was also confirmed from the SD values (in milliseconds), which represent an alternative measure of scatter in the CH distributions of Figure 8. The SD values show that for both the primary fiber and the central neuron, the absolute temporal scatter of responses fell as vibration frequency increased, presumably because the effective dynamic component of the stimulus waveform became more abrupt and therefore better able to synchronize or phase lock the impulse occurrences.

Some variation was seen in the capacity of different pairs to preserve the precise temporal patterning generated in the afferent fibers by these vibrokinesthetic stimuli. For example, for the three pairs in Figure 9, the responses for all three afferent fibers (*dashed lines*) were tightly phase locked, with *R* values of >0.9 at all frequencies from 10 to 300 Hz. However, marked differences are apparent in the capacities of the associated cuneate neurons (*solid lines*) to preserve this tight phase locking. In Figure 9*A*, the preservation was striking, with *R* values of ≥0.87 at all frequencies up to 300 Hz. However, in Figure 9*B*,*C*, the cuneate neuron *R* values declined as a function of frequency, falling to 0.42 at 200 Hz in Figure 9*B* and to ≤0.17 at frequencies of ≥150 Hz in Figure 9*C*, which indicates that phase locking had effectively disappeared in the cuneate responses according to the criteria of Durand and Greenwood (1965). Nevertheless, for many pairs, the preservation of phase locking in postsynaptic responses was striking (Figs. 8, 9*A*) and emphasizes the temporal fidelity of transmission across this cuneate kinesthetic relay. Even in those cases in which double spikes were elicited in the cuneate neuron in response to individual vibration cycles, the pairs of spikes were usually tightly grouped (Fig. 4, 20, 50 and 100 Hz). Thus, the emergence of

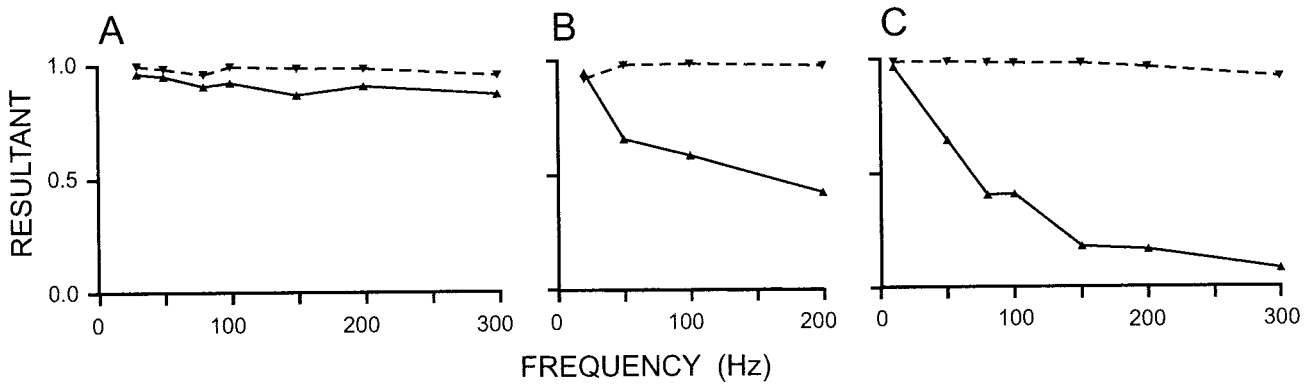

Figure 9. Quantitative evaluation of changes in the tightness of phase locking in responses of three representative wrist joint afferent fiber–cuneate neuron pairs (*A–C*) as a function of the frequency parameter of focal vibratory stimuli applied to the joint capsule. The *dashed lines* plot the vector strength (*R*) derived from the afferent fiber responses, whereas the *solid lines* plot these values for the synaptically linked cuneate neurons. The pair that retained precise temporal patterning in transmission across this synaptic linkage (*A*) also had a high transmission security (e.g., 100% at 50 Hz), whereas those in *B* and *C* that had less faithful retention of temporal patterning had poorer measures of transmission security (40 and 36%, respectively, at 50 Hz).

two-to-one firing need not degrade the fundamental patterning of the response.

Discussion

Location of wrist joint-related cuneate neurons

All 53 cuneate neurons activated by single joint afferent fibers were located in the cluster zone because our recordings were confined to this region. However, the representation of wrist joint input presumably extends over the entire rostrocaudal extent of the cuneate nucleus, because Tracey (1980) recorded from wrist joint-related neurons from ~4 mm rostral to the obex to 5 mm caudal to the obex. Tracey's observed range of response latencies (typically 8–15 msec) overlapped our range of ~5–11 msec. However, he argued that some neurons in his sample may have been activated by indirect, non-monosynaptic input.

Security of transmission for the linkage between single joint afferent fibers and cuneate neurons

The present paired recording study provides the first direct evidence that individual kinesthetic afferent fibers, in this case of joint origin, can exert potent synaptic actions on central target neurons within the ascending pathways concerned with kinesthetic sensory experience. Selective activation of individual joint afferent fibers demonstrated that the minimum sensory input, one impulse in a single sensory fiber, could generate spike output from the cuneate target neuron, which indicates that in this circumstance, the unitary EPSPs generated in the cuneate neuron must be suprathreshold. Because this was observed for 53 wrist joint-related cuneate neurons, we may infer that these potent synaptic linkages between joint afferent fibers and their cuneate target neurons are far from rare. Furthermore, even at input rates in excess of 100 impulses per second, the synapse displayed prominent amplification, because pairs or bursts of cuneate spikes were often generated by individual spikes in the peripheral fiber (Figs. 2–5), which presumably ensured that there was temporal summation at the thalamic level, enhancing the capacity of higher centers for detecting these kinesthetic perturbations. Furthermore, because there is evidence for suprathreshold convergent and divergent actions of joint afferents on cuneate neurons (Coleman et al., 1999a), these attributes could also serve to enhance the transmission efficacy of the afferent signals.

The observations of high security transmission for joint afferents in the cuneate nucleus complement previous findings (Baxendale et al., 1988; Ferrell et al., 1990) of potent reflex actions exerted by knee joint afferents on quadriceps motor units. Although the entrainment of motor units to the joint afferent input was occasionally observed for a single joint afferent fiber, it was usually dependent on activity arising in two or more fibers. Nevertheless, the observations of Baxendale et al. (1988) and Ferrell et al. (1990) emphasize the probable importance of joint afferent input in motor control.

Limitations on transmission efficacy at high input rates

Even with the striking security observed for this linkage, it was found for each pair studied that as input rate increased, a point was reached at which sporadic and then more frequent transmission failures occurred. This may be attributable to afterhyperpolarization, relative refractoriness, and adaptation associated with accumulation of extracellular K^+ ions at these higher levels of activity (Somjen, 1978; Syková and Orkand, 1980; O'Mara et al., 1988) and may also involve presynaptic transmitter depletion (Koerber and Mendell, 1991; Walmsley et al., 1998; Wang and Kaczmarek, 1998). Another explanation could be a conduction failure in the input fiber at some point along the central axon, specifically at branch points at which there may be a low safety factor (Wall et al., 1956; Swadlow et al., 1980; Lüscher et al., 1994). These branch points occur in the dorsal root ganglion, at the spinal cord entry zone, and near the terminal regions of the axon within the cuneate nucleus. However, by recording simultaneously from peripheral and central segments of single afferent fibers (Coleman et al., 1999b), we have found no evidence for propagation failures at either the ganglion or major intraspinal branch points. Nevertheless, for some fibers for which the central intracuneate recording site was near the presumed terminal branches of the afferent axon, there was evidence for sporadic propagation failure into one of the terminal branches at high rates of afferent drive (Coleman et al., 1999b), which suggests that declining cuneate transmission security at very high rates of peripheral drive may be attributable in part to terminal axonal propagation failures, as well as to an actual decline in synaptic efficacy.

Synaptic mechanisms accounting for the high security in the linkage between single joint afferents and cuneate neurons

Although the synaptic terminations of joint afferent fibers within the DCN have not been described anatomically, they may resemble those formed by individual cutaneous or muscle afferent fi-

bers, which are larger and more densely distributed (Rozsos, 1958; Walberg, 1966; Rustioni and Sotelo, 1974; Ellis and Rustioni, 1981; Fyffe et al., 1985, 1986; Weinberg et al., 1990) than those formed by afferent fibers on spinal motoneurons (Redman and Walmsley, 1983). Presumably differences of this kind account for the much larger unitary EPSPs recorded intracellularly in cuneate or in dorsal spinocerebellar tract neurons in response to input from, respectively, single tactile or single muscle afferent fibers (Andersen et al., 1964, 1970; Tracey and Walmsley, 1984) compared with those induced in motoneurons by single muscle afferent fibers (Mendell and Henneman, 1971; Watt et al., 1976; Asanuma et al., 1979; Kirkwood and Sears, 1981; Redman and Walmsley, 1983). Nevertheless, the cuneate unitary EPSPs described in these intracellular studies were subthreshold, in contrast to the indirect evidence for suprathreshold unitary EPSPs in both the present study and our previous studies of cuneate transmission (Ferrington et al., 1987a,b; Vickery et al., 1994; Gynther et al., 1995; Zachariah et al., 2001). The discrepancy may be attributable to damage when the intracellular electrode impales the relatively small cuneate neurons (Andersen et al., 1970).

Implications for kinesthetic coding of secure transmission from single joint afferents to cuneate neurons

The high security of the synaptic linkage formed with cuneate neurons by these single joint afferents meant that many neurons could be driven at high rates (up to 280 impulses per second) by 1-sec-long inputs arriving over a single joint afferent fiber. This allowed the central neurons to display a sensitive grading of response output as a function of changes in presynaptic input rate. Furthermore, the high impulse rates and tight phase locking in cuneate responses to vibratory stimuli (Figs. 8, 9) demonstrated that temporal features of dynamic kinesthetic perturbations, in this case, of a vibratory kind, could be relayed reliably across the cuneate synaptic linkage and preserved with high fidelity in an impulse pattern code.

Although there is no direct kinesthetic counterpart to the tactile vibratory sense, the precision of impulse patterning in joint-related cuneate neurons may be important for kinesthesia, for example, when vibratory or other dynamic perturbations are imposed on the joints in locomotor movements over uneven or unstable surfaces. Furthermore, in human subjects, complex dynamic perturbations for which the precision of impulse patterning in kinesthetic inputs may be crucial will arise in grasping objects, especially moving ones; in the use of serrated cutting devices such as a knife or saw; or in a musical performance that involves the use of the forearm and hand in playing a stringed instrument. In the latter case, the use of vibrato, based on rapid variations in the tone, will impose a vibratory "carrier frequency" on the rapid postural adjustments that take place in the joint while playing the instrument.

Transmission characteristics for single joint afferent fibers: relation to perceptual effects generated by intraneural microstimulation

The present observation that single joint afferent fibers can activate central target neurons of the DCN is entirely consistent with the demonstrated capacity of these fibers to generate a kinesthetic percept, felt as a sense of deep pressure or sense of movement in the associated joint, when activated singly in conscious human subjects after intraneural microstimulation (Macefield et al., 1990). In contrast, selective activation of single muscle afferent fibers almost always fails to generate a kinesthetic percept (Macefield et al., 1990; Ni et al., 1998). However, a similar differential capacity is observed among the different classes of tactile afferent fibers (Ochoa and Torebjörk, 1983; Vallbo et al., 1984). For example, the SAII fibers and many SAI fibers fail to elicit a tactile percept when activated singly, in contrast to PC and rapidly adapting afferent fibers. Presumably, before a contribution can be made to sensory experience by SAII, muscle spindle, or some SAI fibers, there is a need for the concurrent activation of at least a small population of the afferent fiber class before adequate central activation is achieved.

Despite systematic differences among the tactile fiber classes in their capacity for generating tactile percepts, when individual fibers are activated selectively in human microneurography experiments, we have found that all classes of tactile afferents examined (including PC, SAI, SAII, and hair follicle afferent fibers) share a high security of transmission at the DCN relay when tested in a paired recording paradigm (Ferrington et al., 1987a,b; Vickery et al., 1994; Gynther et al., 1995; Rowe, 2001; Zachariah et al., 2001). The present study extends this finding to kinesthetic sources of input by demonstrating that single joint afferent fibers can also exert potent, suprathreshold excitatory actions on DCN neurons. If secure transmission is also found to operate for single muscle spindle afferent fibers, it may mean that the failure of individual SAII, muscle spindle afferents, and some SAI fibers to generate perceptual responses when activated selectively in conscious human subjects may be related to a transmission breakdown at higher levels of the pathway or, for example, to a limited divergence pattern in the central projection, with a failure of the single afferent input to activate the "critical mass" of cortical tissue necessary for perceptual recognition. However, the present observations establish that there is no simple dichotomy between exteroceptive or tactile afferents on the one hand and deep or kinesthetic afferents on the other in their capacity for exerting potent synaptic actions on DCN target neurons.

Finally, we should emphasize that in more physiological circumstances than those that prevailed in the present experiments (for example, in a conscious behaving animal), the transmission characteristics for tactile or kinesthetic inputs to the cuneate nucleus may be subject to modulation from both afferent and descending inhibitory influences (Bystrzycka et al., 1977; Canedo, 1997).

References

Andersen P, Eccles JC, Schmidt RF, Yokota T (1964) Identification of relay cells and interneurons in the cuneate nucleus. J Neurophysiol 27:1085–1095.

Andersen P, Etholm B, Gordon G (1970) Presynaptic and postsynaptic inhibition elicited in the cat's dorsal column nuclei by mechanical stimulation of the skin. J Physiol (Lond) 210:435–455.

Asanuma H, Zarzecki P, Jankowska E, Hongo T, Marcus S (1979) Projection of individual pyramidal tract neurons to lumbar motor nuclei of the monkey. Exp Brain Res 34:73–89.

Baxendale RH, Ferrell WR, Wood L (1988) Responses of quadriceps motor units to mechanical stimulation of knee joint receptors in the decerebrate cat. Brain Res 453:150–156.

Berkley KJ, Budell RJ, Blomqvist A, Bull M (1986) Output systems of the dorsal column nuclei in the cat. Brain Res 396:199–225.

Bledsoe SC, Rupert AL, Moushegian G (1982) Response characteristics of cochlear nucleus neurons to 500 Hz tones and noise: findings relating to frequency-following potentials. J Neurophysiol 47:113–127.

Brown AG (1968) Cutaneous afferent fibre collaterals in the dorsal columns of the cat. Exp Brain Res 5:293–305.

Brown AG, Koerber HR, Noble R (1987) Excitatory actions of single impulses in single hair follicle afferent fibres on spinocervical tract neurones in the cat. J Physiol (Lond) 382:291–312.

Burgess PR, Clark FJ (1969) Characteristics of knee joint receptors in the cat. J Physiol (Lond) 230:317–361.

Bystrzycka E, Nail BS, Rowe MJ (1977) Inhibition of cuneate neurones: its afferent source and influence on dynamically sensitive "tactile" neurones. J Physiol (Lond) 268:251–270.

Canedo A (1997) Primary motor cortex influences on the descending and ascending systems. Prog Neurobiol 51:287–335.

Clark FJ (1972) Central projection of sensory fibres from the cat knee joint. J Neurobiol 3:101–110.

Coleman GT, Zhang HQ, Mackie PD, Rowe MJ (1998a) An intact peripheral nerve preparation for examining the central actions of single kinaesthetic afferent fibres arising in the wrist joint. Prim Sens Neuron 3:61–70.

Coleman GT, Zhang HQ, Rowe MJ (1998b) Transmission security for sustained inputs in the linkage between single joint afferent fibres and cuneate neurones [abstract]. Proc Aust Neurosci Soc 9:27.

Coleman GT, Zhang HQ, Rowe MJ (1999a) Convergence and divergence in the linkages between single joint afferent fibres and their target neurones in the cat cuneate nucleus [abstract]. Proc Aust Physiol Pharmacol Soc 30:117.

Coleman GT, Zachariah MK, Rowe MJ (1999b) Reliable propagation through the dorsal root ganglion of impulses arising in single mechanoreceptive afferent fibres of the cat. Proc Aust Neurosci Soc 10:135.

Coombs JS, Eccles JC, Fatt P (1955) Excitatory synaptic action in motorneurones. J Physiol (Lond) 130:374–395.

Darian-Smith I, Phillips G, Ryan RD (1963) Functional organization in the trigeminal main sensory and rostral spinal nuclei of the cat. J Physiol (Lond) 168:129–140.

Durand D, Greenwood JA (1965) Modifications of the Rayleigh test for uniformity in analysis of two-dimensional orientation data. J Geol 60:229–238.

Ellis LC, Rustioni A (1981) A correlative HRP, Golgi and EM study of the intrinsic organization of the feline dorsal column nuclei. J Comp Neurol 197:341–367.

Ferrell WR, Rosenberg JR, Baxendale RH, Halliday D, Wood L (1990) Fourier analysis of the relation between the discharge of quadriceps motor units and periodic mechanical stimulation of cat knee joint receptors. Exp Physiol 75:739–750.

Ferrington DG, Rowe MJ, Tarvin RPC (1987a) Actions of single sensory fibres on cat dorsal column nuclei neurones: vibratory signalling in a one-to-one linkage. J Physiol (Lond) 386:293–309.

Ferrington DG, Rowe MJ, Tarvin RPC (1987b) Integrative processing of vibratory information in cat dorsal column nuclei neurones driven by identified sensory fibres. J Physiol (Lond) 386:311–331.

Fyffe REW, Cheema S, Light AR, Rustioni A (1985) The organization of neurons and afferent fibers in the cat cuneate nucleus. In: Development, organization, and processing in somatosensory pathways (Rowe MJ, Willis Jr WD, eds), pp 163–173. New York: Liss.

Fyffe REW, Cheema SS, Rustioni A (1986) Intracellular staining study of the feline cuneate nucleus. I. Terminal patterns of primary afferent fibers. J Neurophysiol 56:1268–1283.

Gandevia SC, Burke D, McKeon B (1986) Coupling between human muscle spindle endings and motor units assessed using spike-triggered averaging. Neurosci Lett 71:181–186.

Gordon G, Jukes MGM (1964) Dual organization of the exteroreceptive components of the cat's gracile nucleus. J Physiol (Lond) 179:263–290.

Greenstein J, Kavanagh P, Rowe MJ (1987) Phase coherence in vibration-induced responses of tactile fibres associated with Pacinian corpuscle receptors in the cat. J Physiol (Lond) 386:263–275.

Gynther BD, Vickery RM, Rowe MJ (1995) Transmission characteristics for the 1:1 linkage between slowly adapting type II fibers and their cuneate target neurons in cat. Exp Brain Res 105:67–75.

Hand PJ, Van Winkle T (1977) The efferent connections of the feline nucleus cuneatus. J Comp Neurol 171:83–109.

Horch KW, Burgess PR, Whitehorn D (1976) Ascending collaterals of cutaneous neurons in the fasciculus gracilis of the cat. Brain Res 117:1–17.

Keller JH, Hand PJ (1970) Dorsal root projections to nucleus cuneatus of the cat. Brain Res 20:1–17.

Kirkwood PA, Sears TA (1981) Excitatory post-synaptic potentials from single muscle spindle afferents in external intercostal motoneurones of the cat. J Physiol (Lond) 322:287–314.

Koerber HR, Mendell LM (1991) Modulation of synaptic transmission at Ia-afferent connections on motoneurons during high-frequency afferent stimulation: dependence on motor task. J Neurophysiol 65:1313–1320.

Kuypers HGJM, Tuerk JD (1964) The distribution of cortical fibres within the nuclei cuneatus and gracilis in the cat. J Anat 98:143–162.

Lavine RA (1971) Phase-locking in response of single neurons in cochlear nuclear complex of the cat to low-frequency tonal stimuli. J Neurophysiol 34:467–483.

Lloyd DPC, Hunt C, McIntyre AK (1955) Transmission in fractionated monosynaptic spinal reflex systems. J Gen Physiol 38:307–317.

Lüscher C, Streit J, Lipp P, Lüscher H-R (1994) Action potential propagation through embryonic dorsal root ganglion cells in culture. II. Decrease of conduction reliability during repetitive stimulation. J Neurophysiol 72:634–643.

Macefield G, Gandevia SC, Burke D (1990) Perceptual responses to microstimulation of single afferents innervating joints, muscles and skin of the human hand. J Physiol (Lond) 429:113–129.

Mardia KV (1972) Statistics of directional data. London: Academic.

Matthews BHC (1966) Single fibre activation of central nervous activity. In: Muscle afferents and motor control (Granit R, ed), pp 227–233. New York: Wiley.

McNulty PA, Türker KS, Macefield VG (1999) Evidence for strong synaptic coupling between single tactile afferents and motoneurones supplying the human hand. J Physiol (Lond) 518:883–893.

Mendell L, Henneman E (1971) Terminals of single Ia fibers: location, density, and distribution within a pool of 300 homonymous motoneurons. J Neurophysiol 34:171–187.

Millar J (1979) Loci of joint cells in the cuneate and external cuneate nuclei of the cat. Brain Res 167:385–390.

Ni S, Wilson LR, Burke D, Gandevia SC (1998) Microneurographic stimulation of muscle spindle afferents in the radial nerve fails to elicit proprioceptive sensation. Proc Aust Neurosci Soc 9:183.

Ochoa J, Torebjörk E (1983) Sensations evoked by intraneural microstimulation of single mechanoreceptor units innervating the human hand. J Physiol (Lond) 342:633–654.

O'Mara S, Rowe MJ, Tarvin RPC (1988) Neural mechanisms in vibrotactile adaptation. J Neurophysiol 59:607–622.

Redman S, Walmsley B (1983) Amplitude fluctuations in synaptic potentials evoked in cat spinal motoneurones at identified group Ia synapses. J Physiol (Lond) 343:135–145.

Rowe MJ (2001) Security of central transmission for individual tactile and kinaesthetic sensory nerve fibres. In: Somatosensory processing: from single neuron to brain imaging (Rowe MJ, Iwamura Y, eds), pp 77–100. Sydney: Harwood.

Rozsos I (1958) The synapses of Burdach's nucleus. Acta Morphol Acad Sci Hung 8:105–109.

Rustioni A, Sotelo C (1974) Synaptic organization of the nucleus gracilis of the cat: experimental identification of dorsal root fibers and cortical afferents. J Comp Neurol 155:441–468.

Somjen G (1978) Metabolic and electrical correlates of the clearing of excess potassium in the cortex and spinal cord. In: Studies in neurophysiology: presented to A. K. McIntyre (Porter R, ed), pp 181–201. New York: Cambridge UP.

Swadlow HA, Kocsis JD, Waxman SG (1980) Modulation of impulse conduction along the axonal tree. Annu Rev Biophys Eng 9:143–179.

Syková E, Orkand RK (1980) Extracellular potassium accumulation and transmission in frog spinal cord. Neuroscience 5:1421–1428.

Tracey DJ (1978) The innervation of the knee joint: an anatomical and histological study in the cat. In: Studies in neurophysiology: presented to A. K. McIntyre (Porter R, ed), pp 75–86. New York: Cambridge UP.

Tracey DJ (1979) Characteristics of wrist joint receptors in the cat. Exp Brain Res 305:165–176.

Tracey DJ (1980) The projection of joint receptors to the cuneate nucleus in the cat. J Physiol (Lond) 305:433–449.

Tracey DJ, Walmsley B (1984) Synaptic input from identified muscle afferents to neurones of the dorsal spinocerebellar tract in the cat. J Physiol (Lond) 350:599–614.

Vallbo ÅB, Olsson KÅ, Westberg K-G, Clark FJ (1984) Microstimulation of

single tactile afferents from the human hand: sensory attributes related to unit type and properties of receptive field. Brain 107:727–747.

Vickery RM, Gynther BD, Rowe MJ (1994) Synaptic transmission between single slowly adapting type I fibres and their cuneate target neurones in cat. J Physiol (Lond) 474:379–392.

Walberg F (1966) The fine structure of the cuneate nucleus in normal cats and following interruption of afferent fibres: an electron microscopical study with particular reference to findings made in Glees and Nauta sections. Exp Brain Res 2:107–128.

Wall PD, Lettvin JY, McCulloch WS, Pitts WH (1956) Factors limiting the maximum impulse transmitting ability of an afferent system of nerve fibres. In: Information theory. Third London Symposium (Cherry C, ed), pp 329–344. London: Butterworth.

Walmsley B, Alvarez FJ, Fyffe RE (1998) Diversity of structure and function at mammalian central synapses. Trends Neurosci 21:81–88.

Wang L-Y, Kaczmarek LM (1998) High frequency firing helps replenish the readily releasable pool of synaptic vesicles. Nature 394:384–388.

Watt DGD, Stauffer EK, Taylor A, Reinking RM, Stuart DG (1976) Analysis of muscle receptor connections by spike-triggered averaging. I. Spindle primary and tendon organ afferents. J Neurophysiol 39:1375–1392.

Weinberg RJ, Pierce JP, Rustioni A (1990) Single fiber studies of ascending input to the cuneate nucleus of cats. I. Morphometry of primary afferent fibers. J Comp Neurol 300:113–133.

Zachariah MK, Coleman GT, Mahns DA, Zhang HQ, Rowe MJ (2001) Transmission security for single, hair follicle-related tactile afferent fibers and their cuneate neurons in cat. J Neurophysiol 86:900–911.